β-catenin and canonical Wnts in *Hydra* pattern formation: Insights from mathematical modelling into two distinct systems

Moritz Mercker[1*], Alexey Kazarnikov [1,3], Anja Tursch[2], Stefanie Höger[2], Tobias Lengfeld[2], Suat Özbek [2], Thomas W Holstein[2*], and Anna Marciniak-Czochra[1]

[1] Institute of Applied Mathematics (IAM), Heidelberg University, Heidelberg, Germany
[2] Department of Molecular Evolution and Genomics, Centre for Organismal Studies (COS), Heidelberg University, Heidelberg, Germany
[3] Southern Mathematical Institute of the Vladikavkaz Scientific Centre of the Russian Academy of Sciences, Vladikavkaz, Russia

[*] Corresponding authors. E-mail: mmercker_bioscience@gmx.de and thomas.holstein@cos.uni-heidelberg.de

Abstract

Formation of the body axes and the subsequent formation of the apical termini are fundamental steps during animal development. Nuclear β-catenin and canonical Wnt3 have been identified as major players in both these processes in *Hydra*. Based on molecular knowledge of canonical Wnt signalling directly linking nuclear β-catenin and Wnt3 activity, *de novo* axis formation and head formation have frequently been assumed to be part of the same pattern formation system. In this study, we investigated this relationship by combining new model simulations with available experimental results. We demonstrated that nuclear β-catenin and Wnt3 likely contribute to two distinct *de novo* pattern formation systems in *Hydra*, organizing development and differentiation on two different spatial scales. In particular, the results suggested that nuclear β-catenin acts at the scale of the whole body to control axis formation, whereas canonical Wnt3 signalling is involved in a downstream pathway responsible for small-scale patterning of the head. These results suggest that the underlying mechanisms may also be more complex than previously assumed in other animals where axis formation has been ascribed to canonical Wnt signalling.

Keywords: Pattern formation, *Hydra*, Wnt signalling, Wnt3, β-catenin, mathematical modelling, reaction-diffusion equations, axis formation, head organizer, self-organization

Introduction

Understanding the mechanisms responsible for formation of the primary body axis is a crucial issue in developmental biology [77]. In general, the process is based on maternally derived pre-patterns, such as in the fruit fly embryo [22]. In some cases, axis formation during embryogenesis can be a self-organized process, as demonstrated in various developmental systems ranging from simple metazoans to complex mammalian organs [32,75,84,100,107]. However, even in vertebrate systems, recent data have revealed that spontaneous symmetry breaking occurs in the absence of extra-embryonic tissues [4,98,101]. Consequently, self-organization may serve as a mechanism to ensure the robustness of developed structures under various intrinsic and extrinsic conditions.

Cnidarians are a popular model system for studying general and transmissible principles of development [26,44,51], and the freshwater polyp *Hydra* has been used to study development and regeneration for nearly 300 years. *Hydra* can be used to investigate axis and head formation under different natural and perturbed conditions. In adult polyps, head and axis patterning are constitutively active, to ensure the maintenance of the body axis in a continuous flow of self-renewing and differentiating cells [8–10]. Moreover, the system regenerates –extremities–, such as the head or the foot, as discovered by Abraham Trembley in 1740 [97], and as studied in a range of tissue manipulation experiments [7,71]. Notably, *Hydra* can also regenerate entire polyps from dissociated and re-aggregated cells [32], providing a paradigm for *de novo* pattern formation [83,94]. Furthermore, *Hydra* tissue pieces can be transplanted from a donor to a host polyp by –grafting–, thus providing a model for mutual spatial interactions between tissue pieces from different body regions and thus different morphogenetic

backgrounds [20, 57, 58, 86, 112]. Body axis and head formation also occur during budding, *Hydra*–s asexual form of reproduction, where buds evaginate and grow spontaneously in the budding region of the mother polyp, eventually detaching as functional polyps [76]. Finally, as *Hydra* undergoes sexual reproduction, it also allows the study of the mechanisms driving axis and head formation during embryogenesis [24, 30, 61].

One of the main questions in *Hydra* research is related to the formation, regeneration, and maintenance of the body axis, including the head [25, 34, 90, 104]. The mechanisms driving head and axis formation have been addressed in early grafting and regeneration experiments, which have shed light on the general underlying properties at the tissue level (e.g. [20, 32, 57, 58, 97]). Recent studies identified several candidate molecules involved in these processes, including β-catenin and Wnt3, which were shown to be key players in head and axis formation in *Hydra* [18, 29, 41, 93]. Canonical Wnt signalling has also been studied intensively in a range of model organisms, and Wnt activity, linked to the translocation of β-catenin into the nucleus, was shown to be involved in the control of various developmental processes (reviewed in [3, 50]). These findings led to the conclusion that the canonical Wnt signalling pathway constituted the core structure of the patterning system in *Hydra*. This in turn suggested that Wnt3 and β-catenin were involved in the same pattern formation system, with no distinction between the mechanisms regulating the processes of body axis and head patterning [44, 62, 79, 103].

In addition, *Hydra* has attracted extensive attention for theoretical pattern formation research, starting with the seminal paper by Allan Turing [99], who suggested that specific nonlinear interactions facilitated by different diffusivities could be used to describe the *de novo* formation of patterns, which could be applied to reproduce cutting experiments in *Hydra*. The most famous realization of Turing's idea in a mathematical model of biological pattern formation is the activator-inhibitor model proposed by Alfred Gierer and Hans Meinhardt [31,33,62,64,66]. This abstract model hinted at how complex intracellular pathways coupled to cell-to-cell communication through diffusive molecules could lead to symmetry breaking and the emergence of spatially heterogeneous patterns of gene expression. The activator–inhibitor model and its extensions [6, 11, 56, 60, 69, 85] always assume that both axis and head formation are driven by the same pattern formation mechanism [64, 65]. Based on the molecular knowledge of canonical Wnt signalling, this hypothesis was in agreement with several *Hydra* experiments demonstrating that both nuclear β-catenin and Wnt3 exhibited spatio-temporal correlations; in particular, their expression levels were highest at the oral end of the *Hydra* body column and at the tips of developing buds [8, 9, 17, 29, 41, 44, 52]. Furthermore, pharmaceutical or transgenic induction of nuclear β-catenin induced transient increases in the number of Wnt3 spots [18, 29, 35, 36]. Several studies also showed that Wnt3 mRNA expression depended on β-catenin [74, 79, 103].

In the current study, we conducted a model-based analysis of experimental data, which suggested the existence of two distinct pattern formation systems governing body axis and head formation, respectively. Simulations of models integrating β-catenin and Wnt3 into a single patterning mechanism identified experiments that could not be explained by such a mechanism. This concerns several experiments in which organizer-specific genes are (transiently or permanently) expressed in multiple closely spaced spots. In contrast, in systems based on one single body axis pattern formation only, the distance between organizers is similar to the scale of the body axis, being an obvious contradiction to experimental observations.

Motivated by this discrepancy between the model and experiments, we extended the models of Gierer and Meinhardt to describe the dynamics of nuclear β-catenin and Wnt3 based on two patterning systems connected via the canonical Wnt pathway. We show that β-catenin translocation is involved in the large-scale formation of the body axis, whereas Wnts (in particular Wnt3) drive a distinct small-scale pattern formation system responsible for organizer formation, eventually controlling small-scale head formation downstream of β-catenin. Our results suggest that the control mechanisms may also be more complex in other animals, where canonical Wnt signalling was assumed to drive body axis formation [77], and the small-scale pattern formation processes of the head versus those of the large-scale body axis should not necessarily be identified with each other. In this study, we focused on the core structure of this novel model and provide a systematic justification based on a range of existing experimental results.

Our results offer both, a new theory/paradigm as well as a corresponding fresh view and interpretation of recent and previous experimental data, the latter stemming from various fields of *Hydra* research. As Wnt/β-

catenin mediated pattern formation is fundamental to animal development, our data might also have implications for higher bilaterians, including humans.

Results and Discussion

Experiments contrasting functions of β-catenin and Wnt3 in *Hydra* patterning

Regeneration and grafting experiments

Several tissue-level studies have indicated that head and axis formation in *Hydra* are established by two different patterning systems acting at two different spatial scales. Although both *Hydra* head and body column tissues can lead to ectopic head and axis formation when grafted into a host polyp [9, 17], only the apical part of the head (the hypostome) has organizer capacity and transmits a signal inducing the host tissue to form a secondary axis [17]. Grafted tissue of the body column does not stimulate the surrounding tissue, but self-organizes into a secondary axis composed solely of the transplanted tissue [9, 17, 19, 20]. Furthermore, tissue from the apical tip appears to induce the secondary axis at a much higher frequency [46] compared with grafts from other parts of the body (e.g., [57, 58]). Moreover, even smaller pieces than the hypostome, i.e. clumps of $\tilde{A}\ddot{E} - -10$ epithelial cells derived from the regenerating hypostome, can induce a head axis in reaggregates [93]. All these observations suggest that the processes of axis and head formation originating from the apical tip (small-scale structure) versus tissue of the body column (large-scale structure) must involve different signalling factors [17, 58].

Developmental viewpoint

The existence of two patterning systems acting at different scales to control robust formation of the *Hydra* body plan is also compelling from the developmental point of view. First, *de novo* pattern formation at the scale of the body axis is indicated by the self-organization process during regeneration in *Hydra* aggregates. The resulting body axis gradient is in accord with the experimental observation that transplantation of tissue pieces from the head region is more likely to induce a secondary axis than grafts from more basal regions. The presence of this 'head activation gradient' has been confirmed by several experiments [58]. This property has also been referred to as the 'head inducing potency' [34], gradient of 'head formation capacity' [17], ' -competence' [93], '-potential' [39], '-positional value' [2, 111], and the 'source density' [33, 64].

Second, the head activation gradient has to be subsequently translated into the fine-scale patterning in the *Hydra* head region. Regeneration experiments indicated that the location of head versus foot formation depended on relative, rather than absolute levels of the head activation gradient [7, 8, 71]. Hence, 'direct' translation of the gradient into fine-scale patterns, e.g. based on a threshold mechanisms as originally proposed by Lewis Wolpert [110, 111], is unlikely, because such a mechanism would need to measure very small concentration differences between adjacent cells [63].

In contrast, *Hydra* appears to use a different strategy to realize the transition from large- to small-scale patterns: the head activation gradient (co-localizing with *nuclear β-catenin/T-cell factor* (*Tcf*) expression) creates a small organizing spot ('head organizer') defined by *Wnt3* expression [9, 10, 18, 41], which is in turn localized at maximal (or sufficiently high) levels of nuclear β-catenin/Tcf [41, 93]. The organizer spot is assumed to control the stepwise construction of the *Hydra* head, including the tentacles [7, 10, 13, 17, 52]. However, grafting experiments [17] and studies of *Hydra* aggregates [41, 93] suggest that the relationship between the large-scale body axis system and the small-scale organizer system is probably bidirectional. In particular, local expression of head/organizer-specific 'point source genes' (such as *Wnt3* or *HyBra*) are assumed to direct/restrict the large-scale expression patterns e.g. of *β-catenin/Tcf* [93].

In summary, instead of the possibly non-robust direct transformation of the large-scale gradient into small-scale patterns, the large-scale body axis gradient seems to be involved in mutual positive feedback with another, small-scale patterning system defining the head organizer. Robustness is thus achieved via redundant mechanisms (acting at different scales), which is a well-known principle in various biological contexts [105].

Single-gene expression studies

In situ hybridization- and green fluorescent protein (GFP)-based reporter gene studies revealed that although *β-catenin* and *Wnt3* were co-localized with respect to their maxima, they were expressed at different spatial scales: *β-catenin* (and the associated *Tcf*) showed diffuse expression patterns matching the scale of the body axis, whereas expression of *Wnt3* and all other *Hydra Wnt* genes always occurred in small spots [18, 29, 41, 45, 52, 92, 93]. The activities of these two factors differed not only in their spatial patterns, but also in their dynamics. Except for experiments involving tissue injury that may trigger *Wnt3* expression directly [104], evidence suggests that *Wnt3* is expressed at later stages than *β-catenin/Tcf*. *Wnt3* expression was distinctly delayed compared with *β-catenin/Tcf* during embryogenesis [24] and during budding, with *Wnt3* expression coinciding with the first bud protrusions [41], while *β-catenin/Tcf* expression was already evident prior to the first visible deformations [45,106]. Indeed, inhibition of *β-catenin* prevented bud formation, including the expression of several bud- and organizer-specific genes [106]. In summary, the results of these spatial and temporal expression studies suggest that the activities of both molecules are controlled by different mechanisms acting at different spatio-temporal scales, with *Tcf/β-catenin* frequently preceding *Wnt3* expression.

Transcriptomic analyses and signalling pathways

Recent progress in our understanding of canonical Wnt signalling in different animals provides a direct link among secreted Wnt molecules, nuclear β-catenin, and Tcf transcription factors [3, 50, 74]. This has led to the widespread assumption that β-catenin/Tcf and Wnt3 must act within the same pattern formation system, with the secreted Wnts at the core of this system [106]. However, the observation that *Wnt3* expression requires nuclear β-catenin/Tcf does not imply that the body-scale pattern formation system coordinated by β-catenin/Tcf relies on Wnt3. On the contrary, while Wnt3 function is associated with the head organizer [9,10,18,41], β-catenin/Tcf-dependent signalling is involved in diverse molecular, non-molecular, intrinsic and extrinsic processes. Its role is thus versatile and fundamental: it is required for the early regeneration response and pre-patterning [37], and controls the expression of approximately 1000 different genes, including several components of the bone morphogenetic protein, Notch, and transforming growth factor-β pathways, several transcription factors, as well as genes influencing cell-cell adhesion, cytoskeletal components, and the extracellular matrix (ECM) [79, 106]. With specific regard to *Hydra* axis formation, the nodal-pitx cassette has been shown to act under the control of β-catenin [106]. Moreover, β-catenin appears to be a required co-factor for establishing biradial budding asymmetry [106]. In addition to its role as an important transcriptional co-factor in cell nuclei, the membrane-associated distribution of β-catenin in other body regions indicates a function in *Hydra* tissue mechanics [21, 41, 42, 45], such as in cell-cell adhesion [73]. Furthermore, *β-catenin* expression levels have recently been linked to ECM elasticity [102], which in turn plays an important chemical and mechanical role during pattern formation and regeneration. External biotic and abiotic environmental cues have also recently been shown to affect β-catenin-mediated signalling and pattern formation [12, 91]. The complexity of β-catenin/Tcf-related processes suggests that β-catenin-dependent *Wnt3* expression is only one of several pattern formation loops activated by gene expression downstream of β-catenin/Tcf [74, 106], thus making *Wnt3* expression dispensable in terms of body axis formation. Recent experimental evidence of this dispensability is given by experiments where *Wnt3* expression (and thus head formation) is suppressed, but foot development indicates the self-organization of a body axis in *Hydra* aggregates [23].

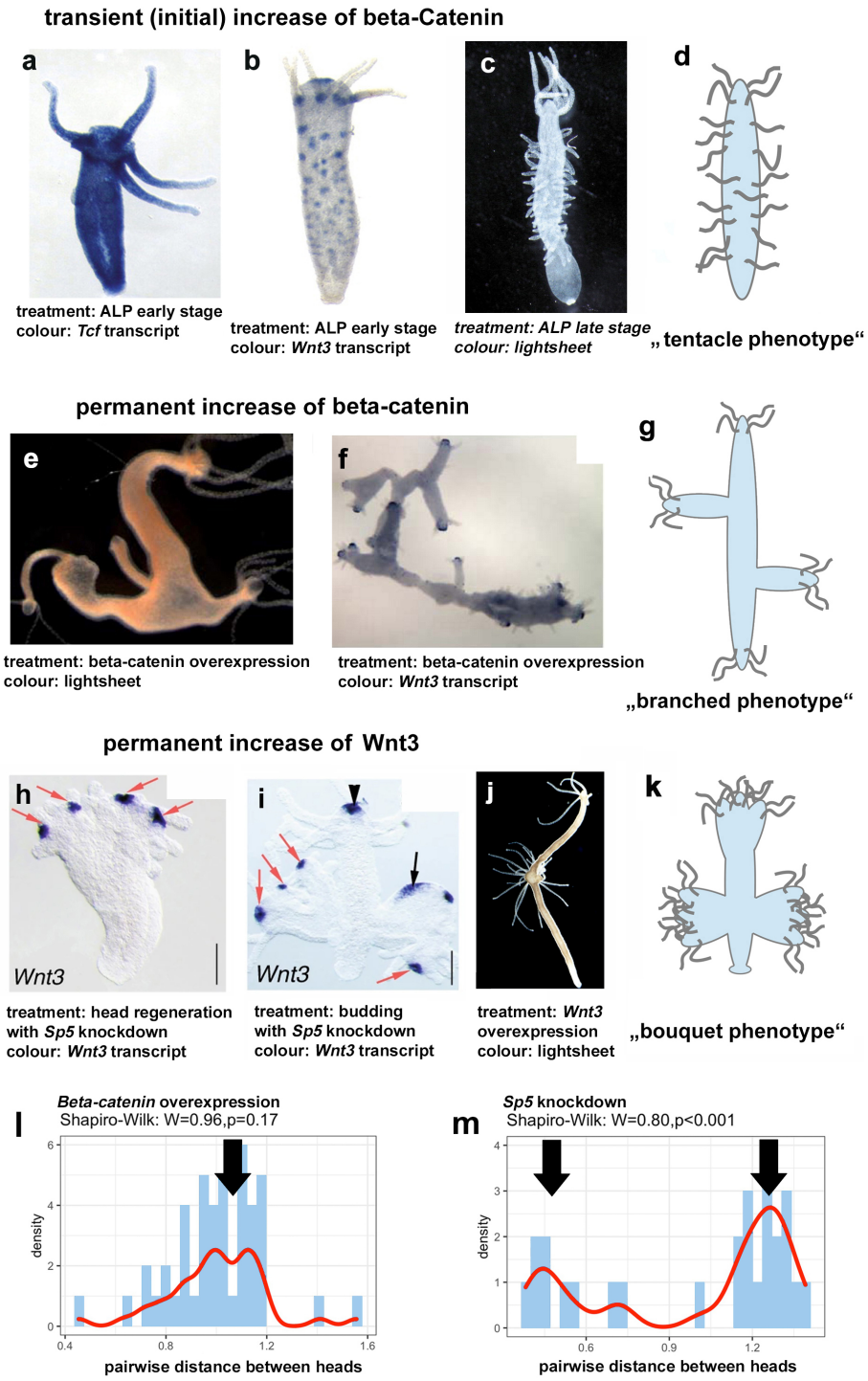

Figure 1. Experimental data (a–c, e–f, h–j) and sketches of phenotypes (d, g, k) resulting from a transient increase in β-catenin/Tcf (a–d), a permanent increase in β-catenin/Tcf (e–g), and a permanent increase in Wnt3 (h–k), respectively. (l–m): histograms (blue) and density plots (red) of pairwise distances between heads of polyps with increased *β-catenin/Tcf* (l) respectively *Wnt3* (m) expression. Black arrows indicate the different modes. (a–c) are modified from Ref. [18], (e–f) from Ref. [29], and (h–i) from Ref. [103] (the latter published under the Creative Common license).

Molecular manipulations and multi-headed phenotypes

RNAi or transgenesis techniques have opened the way for the analysis of *Hydra* phenotypes resulting from the body-wide overexpression or knockdown of single genes [55, 109]. In particular, *β-catenin* knockdown [103] and overexpression [29] have been studied in *Hydra* lines. *Wnt3* overexpressing lines are also available [114], and knockdown of putative Wnt3 inhibitors has recently been carried out. Inhibitors can act directly at the level of transcriptional regulation or by interference with Wnt ligands, such as the Wnt antagonist Dickkopf (Dkk 1/2/4) [2, 36, 68], Sp5 [103], and the Wnt-specific protease HAS-7 [114]. As expected, overexpression (direct or indirect resulting from inhibition of an inhibitor) of either *β-catenin* or *Wnt3* produced phenotypes with multiple heads (c.f., Fig. 1 e–k). However, a more detailed examination of these phenotypes allowed the distinction of two different categories. A permanent increase in Wnt3 (either directly through overexpression [114], or indirectly by *Sp5*- [103] or *HAS-7* knockdown [114]) frequently resulted in animals with multiple heads, located in close proximity to each other ('bouquet phenotype' – Fig. 1 h–k). In *Sp5* RNAi animals, these ectopic heads/axes occurred particularly at the oral pole or in the budding zone, where β-catenin/Tcf levels were high [103]. The same occurred in *Wnt3* overexpressing animals, though the ectopic head locations were more variable. In contrast, a permanent increase in β-catenin resulted in animals with regular branches of new axes, with a normal distance between the head and budding zone ('branched phenotype' – Fig. 1 e–g). Further experimental support for the existence of these two phenotypes is obtaned by the statistical analysis of the pairwise distances between the heads in polyps with manipulated β-catenin respectively *Wnt3* levels: polyps with increased *β-catenin* expression show an unimodal histogram plot not significantly deviating from a normal distribution (Shapiro-Wilk test: $W = 0.96, p = 0.17$ – Fig.1 l), whereas polyps with increased *Wnt3* levels show a bimodal histogram strongly deviating from the normal distribution (Shapiro-Wilk test: $W = 0.80, p < 0.001$ – Fig.1 m). More details on this analysis are given in the supporting information S1. Thus the phenotypes resulting from overexpression experiments and observations at the tissue level indicated that secreted Wnt3 and cytoplasmic/nuclear β-catenin/Tcf mediated different aspects of *Hydra* patterning.

Interestingly, a non-permanent increase in β-catenin/Tcf using a high dose of alsterpaullone (ALP) did not lead to the formation of multiple axes, but rather resulted in transient expression of multiple *Wnt3* spots all over the body, followed by the formation of ectopic tentacles [18, 29] (Fig. 1 a–d). The combination of ALP treatment with *Wnt3* knockdown led to a reduction in the number of ectopic tentacles, demonstrating that β-catenin and Wnt3 exert distinct but complementary functions in axis formation [54]. Finally, administration of a lower dose of ALP for a longer time also led to ectopic axes, similar to the *β-catenin* overexpression phenotype described above [114].

Computational approach to study the functions of β-catenin versus Wnt3

Mathematical setting

We propose a mathematical model describing the dynamics of the different signalling components in the *Hydra* patterning system to obtain mechanistic insights into their roles. The model is given in terms of partial differential equations (PDEs) accounting for spatio-temporal interactions among the signalling factors defined on an evolving domain representing the tissue. Application of a continuous modelling approach was justified by the large number of cells ($\geq 5 \times 10^4$) in the system [96]. To account for the realistic geometry of the *Hydra* tissue bilayer, we adopted a mechanochemical modelling approach as proposed in Ref. [67, 69, 70]. We assumed that reaction-diffusion equations describing the signalling system were defined on a curved two-dimensional (2D) surface embedded in a 3D space. The geometry of the curved surface evolved over time according to a gradient-flow of Helfrich-type energy reflecting the fact that bending of the tissue away from a preferred local curvature was energetically unfavorable. We assumed that small tissue deformations, e.g. in the initial phase of tentacle development, followed patterns of gene expression. In contrast to the fully coupled mechano-chemical model of [69], in the main version of our presented model (for an mechanochemical alternative, c.f., below) we did not consider any feedback between the mechanical properties of the tissue and the gene expression processes. The reason is, that in Ref. [69], we considered axis formation in mechanically oscillating *Hydra* re-aggregates of dissociated cells, which are systems that were described to require mechanics for patterning. In the current paper, in contrast, we focus on axis vs head formation in *Hydra*, which also comprises processes such as head regeneration, homeostasis, and budding. However, for now, it remains unclear whether the mechanical stretching in aggregates is not an "artefact" of the

sphere-like reaggregates lacking a preformed mouth opening which is characteristic for intact animals, so that the mechanical stress is possibly not essential for *Hydra* axis formation in general. Thus, for the sake of simplicity, we neglect the role of tissue stretching for now. Consequently, the pattern formation process was based solely on molecular interactions. The choice of model geometry was motivated by a realistic description of the tissue as a radially symmetrical ellipsoid undergoing small deformations due to changes in gene expression patterns.

To demonstrate the robustness of the presented idea, we developed and presented a second version of our model, relying on similar qualitative interactions between the different pattern formation systems, but using completely different mechanisms for β-catenin and Wnt3 *de novo* pattern formation itself (c.f., supporting information S3). Since there is increasing evidence that tissue mechanics may actively influence axis formation [14, 53, 69] particularly *Wnt3* expression [23] in *Hydra*, here, instead of using an activator-inhibitor-type mechanism, we adapted and applied the mechanochemical patterning mechanism as presented in Ref. [67]. Furthermore, for the *de novo* formation of the body axis, we replaced the Turing mechanism by the mutual inhibition (MI) model as recently presented by [68] (more details are given in the supporting information S3).

Details of the mathematical setting are provided in the 'Materials and Methods' section. The remainder of this section focuses on the mathematical modelling of *Hydra* signalling, the biological justification of the model structure, and model validation based on the experimental data.

Mathematical model to test the hypothesis that β-catenin and Wnt3 control two distinct pattern formation systems

The simplest explanation of the spatio-temporal differences between localized *Wnt3* expression and body column scale *β-catenin/Tcf* patterns could be provided by a mechanism in which β-catenin/Tcf forms part of a signalling loop exhibiting *de novo* formation of a pattern, with *Wnt3* expression being activated above a certain β-catenin/Tcf threshold. Indeed, such a mechanism has been proposed in Ref. [64, 65], where Wnt3 was locally amplified due to an additional loop to explain the scale difference in *Wnt3* versus *β-catenin* expression spots. Consequently, it was not explicitly distinguished between the axis and the head formation. However, a systematic simulation study of the model from Ref. [64, 65] reveals that it is not capable of producing stable *Wnt3* patterns, but *Wnt3* spikes grow unbounded in time (c.f., supporting information S2). To further investigate this idea, we reduced the complexity of this model by assuming *Wnt3* expression above a certain critical β-catenin level (without controlling an autonomous patterning system), and assuming an activator-inhibitor model for β-catenin patterning, but without the additional molecular complexity of the model presented in Ref. [64, 65]. Simulations of ALP-treatment reveal that this model is not able to explain the experimentally observed transient *Wnt3* spots (c.f., below, as well as supporting information S3).

However, several experimental observations have suggested that Wnt3 drives a partially autonomous pattern formation system, rather than being just a read-out of β-catenin/Tcf activity. Clues regarding the complexity of the system are provided by pharmaceutical manipulations using ALP. ALP prevents β-catenin degradation, resulting in a high, body-wide, constant level of *β-catenin/Tcf* transcript (Fig. 1 a). Interestingly, this pattern is not followed by *Wnt3*, which is expressed in a complex arrangement of multiple organizer-sized spots all over the body (Fig. 1 b) [18, 29, 35, 36, 41, 103]. This confirms that increased activity of β-catenin/Tcf resulted in increased production of Wnt3, but likewise demonstrated that its spatial dynamics were affected by an additional regulation mechanism, leading to qualitatively different expression patterns of the two factors, which act at distinct spatial scales. Notably, even a broad domain of β-catenin/Tcf activity resulted in strictly localized Wnt3 patterns (with preserved spot size), and may hence provide precise instructions for the process of head formation. In contrast, the threshold mechanism suggested by Wolpert would result in an increase in size of the Wnt3 spots, leading to body-wide constant *Wnt3* expression in the event of strongly elevated β-catenin/Tcf levels. In fact, the observed restricted *Wnt3* expression spots indicated the existence of a mechanism providing robust organizer formation. In particular, it prevented an increase in the *Wnt3* expression domain, which seems to be important for proper head-organizer function. It is therefore unlikely that formation of the head organizer depends solely on β-catenin/Tcf activity, considering the variety of extrinsic and intrinsic factors modulating β-catenin/Tcf levels in *Hydra*, e.g. [12, 37, 45, 79, 91, 102].

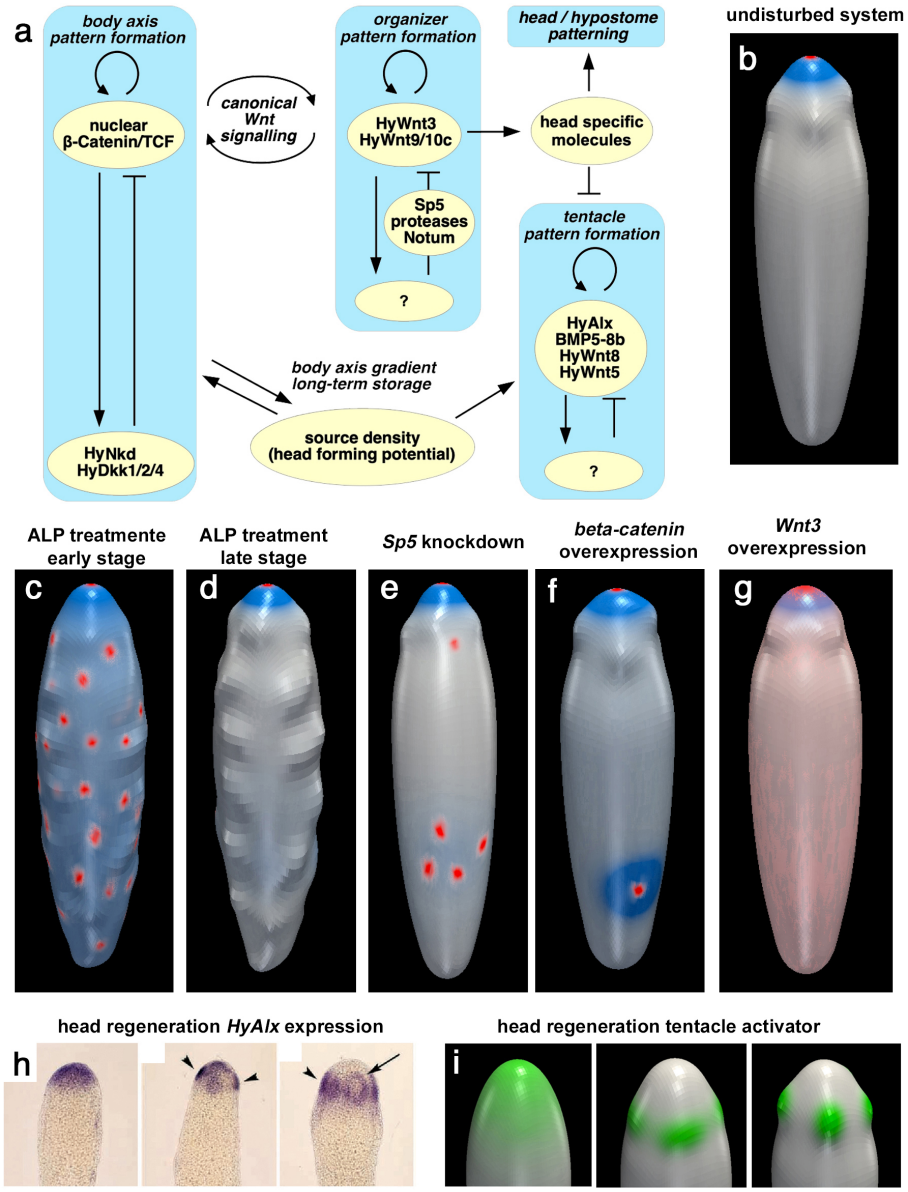

Figure 2. Scheme (a) and simulation results (b–g, i) of the novel *Hydra* pattern formation model assuming distinct pattern formation systems for the body axis including β-catenin/Tcf [29, 41], the head organizer including Wnt3 and Wnt9/10c [78], and the tentacle system including Wnt5, Wnt8, HyAlx, and BMP5-8b [78, 80, 87]. Red colour in (b–g) indicates high local levels of Wnt3/Wnt9/10c and blue indicates high local levels of β-catenin/Tcf. Color scaling is similar in all simulation snapshots. Developing tentacles are indicated by local tissue evaginations. The lower panel presents the time series of experimentally observed *HyAlx* expression during head regeneration (violet color in (h) - figure adapted from Ref. [87]) and tentacle activator marker during simulations (green colour in (i)).

Based on the above considerations, we formulated a new mathematical model of symmetry breaking and pattern formation in *Hydra*, which could reproduce the dynamics of β-catenin/Tcf and Wnt3 activities. The aim was to determine if the existence of additional control of Wnt3 patterns was sufficient to explain the experimental observations, and to provide a core model of *Hydra* development and regeneration that could subsequently be extended and applied to address new experimental questions. The proposed model is an extension of the well-established Gierer–Meinhardt model, and accounts for three pattern formation subsystems describing (1) a pattern formation system of the body axis gradient, (2) a separate pattern formation system for the head/organizer, and (3) a patterning system describing tentacle developent. Additionally, these systems are assumed to interact with the well-known long-term storage of the body axis gradient (head-forming potential / source density [64]). The novelty of this model is that we zoomed out the head/body axis patterning system and explicitly distinguished between two (interconnected) pattern formation systems acting differently in the apical region versus the body column. We assumed that the body-scale pattern formation system was informed by nuclear β-catenin/Tcf, which, among others, activated the production of Wnt3, which was in turn additionally mediated by an independent control loop providing head organizer function on a small scale. A scheme of the model is presented in Fig. 2. Specific interactions between model components, assumptions about model parameters, initial conditions, and information on the simulation code and software are given in the 'Materials and Methods' section.

The core structure of the β-catenin/Tcf and Wnt3 patterning systems was based on the activator–inhibitor signalling loop exhibiting Turing instability. For simplicity, we assumed that Wnt3 formed part of a signalling loop with a hypothetical Wnt3 inhibitor. The latter can be linked to the recently discovered Sp5 transcription factor, which plays an important role in the transcriptional inhibition of Wnt3 [103]. Notably, the antagonistic interactions may also occur on different levels. In addition to Sp5, we identified other well-established Wnt antagonists that exhibit synexpression with the putative gradient-like Wnt action domains, including transcripts that encode naked cuticle (Nkd), which binds to the Dishevelled (Dvl) family of proteins preventing the translocation of β-catenin into the nucleus [81,108]. Notum, as another Wnt antagonist, is a palmitoleoyl-protein carboxylesterase that requires glypicans to suppress Wnt signalling by depalmitoleoylation of Wnt proteins [47,48]. Furthermore, this complex network of Wnt antagonists might even include Wnt inhibitors that act by cleaving Wnts to inactivate specific Wnt ligands [113,114]. It is striking that some, such as Nkd, have demonstrated both negative and positive regulatory effects on Wnt signalling in insects and mammals, and have been shown to exert feedback control in a context-dependent manner [28]. Accounting for these molecular details would significantly increase the model complexity, beyond the scope of this paper. Consequently, the proposed model did not take account of the molecular details of Wnt3 interactions. The applied activator–inhibitor framework should thus be considered rather as an approximation of the *de novo* pattern formation mechanism, which is still not fully understood at the molecular level. In this context, the desired dynamics may emerge not only from chemical processes (such as activator–inhibitor coupling), but also from mechano-chemical, cellular, and bio-electrical processes [14,53,69,82,89].

Model simulations and comparison with experimental data

We simulated a steady-state system and a system challenged by ALP treatment, knockdown, or overexpression in order to identify an appropriate set of model components involving Wnt3 and β-catenin/Tcf that could explain the observed patterns. We demonstrated the need for a supplementary regulatory mechanism of Wnt3, because a single pattern formation system (as in the Gierer–Meinhardt models) was insufficient to explain the experimental outcomes of different manipulations of the β-catenin/Tcf and Wnt3 systems. Thus, the assumption that head and body axis are based on independent pattern formation systems is necessary to explain a wide variety of experiments, but we aim to keep the model minimal in the sense that the *de novo* patterning processes of the two distinct systems are not modelled in the molecular detail (partially for reasons of model complexity, partially because corresponding molecular information is still missing). Below, we discuss the results of the models and their limitations in the context of different experimental scenarios.

We first checked that the model described the steady-state scenario adequately. The simulations (Fig. 2 b) showed spontaneous development of the head. The resulting gradient-like patterns of *β-catenin/Tcf* expression, with a maximum at the head, a small and sharp spot of *Wnt3* expression at the tip of the hypostome, and a

ring of tentacles beneath the head, were in agreement with experimental observations [41]. The dynamics of the appearance of the tentacle-related patterns also resembled previous experimental observations (compare Fig. 2 h and Fig. 2 i).

As previously discussed, these aspects of head establishment were also captured by previous models considering only a single pattern formation system for body axis and head formation [64, 87]. We therefore carried out further model validation based on the ALP experiments. Simulations with initial conditions corresponding to ALP treatment reproduced the experimentally observed patterns described e.g. in [18, 29] (see Fig. 1 a–c). In the early stages after ALP application, we observed an increase in β-catenin/Tcf levels in the entire body column accompanied by multiple Wnt3 spots (Fig. 2 c). Subsequent expression patterns of *β-catenin/Tcf* and *Wnt3* resembled those of the steady-state system, with the additional development of ectopic tentacles at the body column (Fig. 2 d). Furthermore, simulations including knockdown of the Wnt3 inhibitor led to multiple Wnt3 spots in both the head region and the budding zone (Fig. 2 e), in accordance with observations of adult polyps and head regeneration following *Sp5* knockdown (Ref. [103], c.f. Fig. 1 h–i). Interestingly, in the late stages of these simulations, ectopic Wnt3 spots vanished (not shown), whereas in real experimental systems, they developed into ectopic heads [103]. Nevertheless, the ectopic Wnt3 spots persisted significantly longer in the simulated *Sp5* knockdown model compared with simulations including ALP treatment. We concluded that a certain morphogen synthesis time is required in the real system, sufficient to initiate a local cell differentiation process. The latter leads to 'fixation' of the organizer and demonstrates that a transient expression pattern is sufficient to control the process. These effects were not incorporated in our present and previous models. Finally, we compared the model to experiments based on *β-catenin* overexpression [29]. The model correctly predicted the formation of one or multiple ectopic body axes at much larger distances from each other compared with the *Sp5* knockdown phenotype (Fig. 1 e–f).

The only disagreement between the model and experimental observations occurred for the simulated scenario of *Wnt3* overexpression. Simulations of the corresponding model with an additional constant Wnt3 production resulted in a body-wide increase in Wnt3 combined with a larger Wnt3 spot at the upper hypostome (Fig. 2 g). In contrast, experiments showed the development of multiple heads at varying positions (Fig. 1 j). This qualitative difference between the simulations and experimental results may be related to the properties of the activator–inhibitor model responsible for the *de novo* pattern formation mechanism in our model. However, it can be shown mathematically for a general class of reaction–diffusion pattern formation systems (including the activator–inhibitor model) that a uniform increase in activator production cannot change the shape of the pattern. Thus, the multi-headed phenotype seen in the *Wnt3* overexpression experiment cannot be explained by such models and a more refined model is needed. Identifying the exact underlying chemical/physical mechanisms on the molecular level is however beyond the scope of this work. Yet, we can demonstrate that in general, the mechanism of *de novo* pattern formation exhibited by the activator-inhibitor model (and several related models) describes Wnt3 spot formation only to a limited extent, and most possibly additional mechanisms are at work here. As demonstrated in the supporting information S3, completely different Wnt3 *de novo* patterning mechanisms may lead to similar simulation results. However, this finding does not limit our main conclusions, namely the existence of two partially independent pattern formation systems for axis versus head formation.

Summary and Outlook

In this study, guided by a systematic analysis of available experimental data, we proposed a new mechanism and corresponding mathematical model of head and body axis formation in *Hydra*. We integrated the results of diverse experimental approaches and data sets, including regeneration and grafting experiments, molecular/chemical manipulations leading to multi-headed phenotypes, analysis of single-gene expression patterns, and transcriptomic data related to β-catenin and Wnt. We observed that β-catenin/Tcf and Wnt3 act qualitatively differently in *Hydra* in distinct/various spatial, temporal, and experimental contexts, suggesting the need for independent control mechanisms.

We therefore proposed a mechanism in which the core system controlling formation of the body axis gradi-

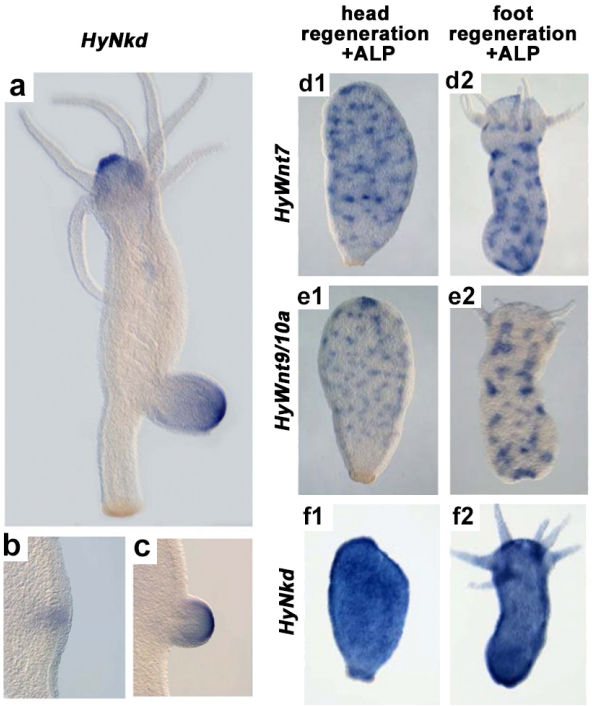

Figure 3. Experimental comparison of large-scale diffusive expression patterns and small-scale spotty expression patterns of different genes suggesting their involvement in the two different patterning systems. (a–c) Analysis of large-scale expression patterns of *HyNkd* in adult polyps, suggesting that HyNkd is involved in the large-scale β-catenin-based patterning system; (d–f) formation of distinct patterns (diffusive versus spotty) in animals treated with 5 μM ALP, evaluated after 72 h, suggesting that expression levels of multiple *Wnts* (d1,d2,e1,e2) are regulated differently from HyNkd (f1,d2).

ent is based on β-catenin/Tcf, while Wnt3 is involved in an extra pattern formation system acting at a small spatial scale, which locates and defines the head organizer. Both systems are tightly coupled via canonical Wnt signalling. Thus, there are two largely independent patterning systems for head versus axis formation. *Wnt3* and β-catenin appear to contribute to clearly different developmental processes and, although acting in the same signaling pathway, they do not have to act together. This is a paradigm shift with a strong potential influence on future experimental work. The idea is significantly new and thus not yet present in the experimental community as it can be seen by the fact that even several recent papers investigating the molecular basis of Hydra patterning notoriously do not distinguish between axis versus head formation.

To test the performance of the proposed two-scale Wnt3/ β-catenin patterning mechanism, we implemented these systems in a mathematical framework of reaction–diffusion equations. The model was based on an extension of the seminal Gierer–Meinhardt model (e.g., [62, 64]), in which the *de novo* patterning mechanism is provided by a Turing-type activator–inhibitor loop. In contrast to previous models, we explicitly distinguished between a system defining the large-scale formation of the body axis defined by a gradient of β-catenin/Tcf activity and the mechanism of head formation localized by Wnt3. To account for the realistic geometry of the *Hydra* tissue bilayer, we adopted a modelling approach coupling morphogen dynamics with the evolution of a deforming tissue. Model simulations demonstrated the ability of the proposed model to explain a range of experimental observations that could not be described by a classical single activator–inhibitor loop. The model results were consistent with transient and stable *Wnt3* expression patterns following ALP treatment, *Sp5* knockdown, and *β-catenin*

overexpression.

The only disagreement between the simulations and experiments was related to *Wnt3* overexpression, for which experiments showed a transition from a gradient-like pattern to a multiple-spot (ectopic heads/axes) structure [114], while model simulations predicted a homogeneous body-wide increase in Wnt3. These dynamics cannot be obtained in a general activator–inhibitor model by an increase in activator production, thus highlighting the limitations of the activator–inhibitor mechanism. Mathematical understanding of this disagreement is an important step towards the identification of a more plausible pattern formation mechanism. Further extensions of the model require more careful experimental investigations of the molecular interactions, accounting for Sp5 [103], HAS-7 [114], and other Wnt antagonists.

Our conclusions regarding the co-existence of two different regulatory mechanisms controlling body column and head formation are also supported by experiments showing the co-existence of distinct types of patterns for different genes under the same treatment (see Fig. 3). Figure 4 provides an experimental setting for the allocation of molecular candidates to either the large-scale body axis or small-scale organizer in *Hydra*. Specifically, it links patterns exhibited by the putative Wnt/β-catenin inhibitor Nkd to those observed for β-catenin/Tcf [37, 41, 45], suggesting that this molecule is involved in the body axis gradient system. *HyNkd* expression during budding (Fig.3 b–c) further revealed that this gene is already expressed during the early stages of budding and regeneration, indicating a role during the basic pattern formation process. Analysis of expression patterns after ALP treatment confirmed these assumptions, with *HyNkd* expression (f1–f2) showing a homogeneous body-wide pattern, similar to the expression pattern of *β-catenin/Tcf* [18, 29] but significantly distinct from the spotty, small-scale patterns of multiple *Wnts* (d1, d2, e1, e2). Indeed, Nkd has been shown to be a widely conserved feedback regulator preventing the translocation of β-catenin into the nucleus (by interacting with Dishevelled and Axin) [28, 108], thus primarily affecting β-catenin signalling, whereas Wnt signalling is only affected indirectly.

Interestingly, recent experiments indicated that, in addition to diffusing chemicals, physical cues such as discrete cellular nearest neighbour interactions [13, 27, 49, 72, 88], tissue mechanics [14, 53, 69, 89], and bio-electrical processes [15] all contributed actively to pattern formation in *Hydra*. The integration of non-diffusive and diffusive signals thus offers a viable alternative to the classical Turing theory of *de novo* pattern formation and may have important consequences for experimental studies.

In summary, the molecular basis of canonical Wnt signalling established in previous decades [3, 43] clearly indicated that the Wnt signalling pathway plays an outstanding role during head and axis development, not only in *Hydra* [41], but also in other higher organisms [77]. However, previous models did not distinguish between body axis and head formation in the context of canonical Wnt signalling. In contrast, employing a combination of mathematical modelling and simulations using the available experimental data, the current study provides the first evidence indicating that these two systems are controlled by two distinct self-organizing processes. These two systems are coupled via the canonical Wnt signalling pathway, which ensures continuous alignment of the head with the body axis.

Although accounting explicitly for Wnt3 and β-catenin/Tcf, the proposed model involves hypothetical inhibitors that might be linked to the Sp5 transcription factor [103] or HyDkk1/2/4 [2, 36, 68]. Refinement of the model to account for the molecular details of the underlying mechanisms would significantly increase the model's complexity, and we therefore formulated the basic Wnt3/ β-catenin model in terms of a reduced mathematical representation of the underlying mechanisms. Moreover, numerous studies of different pattern formation mechanisms have demonstrated the difficulty of distinguishing among them at the level of basic experimental data, thus highlighting the need for more-detailed molecular information to identify the plausible mechanism. The proposed mathematical model provides a tool to guide the respective experimental research and interpret its results.

In 2012, based on over 40 years of research into *Hydra* pattern formation, Alfred Gierer noted that even detailed knowledge of the molecules involved in *Hydra* pattern formation was not sufficient to explain the resulting spatial structures [31]. We posit that the patterns arise as an emergent effect that can be understood from an interdisciplinary perspective, integrating different chemical and physical processes and principles at the molecular, cellular, and tissue scales [14, 31]. Further refinement of our models by integrating the results of different biolog-

Variable name	Explanation
β_cat	nuclear β-catenin/TcF
β_cat_{ant}	β_cat antagonist (presumably linked to Dickkopf1/2/4-C [2, 64, 68] or HyNkd)
$Wnt3$	Wnt3 (possibly also involving Wnt9/10c [52])
$Wnt3_{ant}$	Wnt3 antagonist (related to Sp5 [103], HmTSP [54], or Notum signaling)
$Head$	Head-related factors downstream of Wnt3 (e.g., multiple Wnts [52])
SD	Source density (long-term storage of the head-forming potential)
$Tent$	Tentacle activator (may involve HyAlx [87], Wnt8, and Wnt5 [78] or BMB5-8b [80])
$Tent_{ant}$	Tentacle activator antagonist (unknown)

Table 1. Model variables and their biological interpretation.

ical, biophysical, and biochemical disciplines will help to unravel the mechanisms driving self-organized pattern formation during development, as one of the mysteries of biology.

Materials and Methods

Definition of the model domain

The cell bilayer is at any time t approximated by a closed 2D surface ellipsoid $\Gamma(t)$, embedded in 3D space. The evolution of $\Gamma(t)$ is given by a diffeomorphic time-dependent representation $\vec{X}$, parameterized over the unit sphere $S^2 \subset \mathbb{R}^3$. Thus, $\Gamma(t)$ is the image of $\vec{X}(\cdot, t)$ with $\vec{X}(\vec{s}, t) : S^2 \times [0, T] \to \mathbb{R}^3$ for a $T \in \mathbb{R}_{>0}$. Local concentrations of different gene products at time t are given by a set of continuous functions Φ_i, $i = 1, ..., n$, on the deforming tissue surface $\Gamma(t)$, defined as gene product concentrations per cell volume, $\Phi_i(t) : \Gamma(t) \to \mathbb{R}_{\geq 0}$. In order to achieve a consistent formulation with chemical processes being defined on S^2 rather than on Γ, we redefined Φ_i accordingly. This can be achieved based on the fact that we can identify material points $\vec{X}(\vec{s}, t)$ on $\Gamma(t)$ with $\vec{s} \in S^2$, because $\vec{X}$ is smooth and bijective. Thus, for each $\vec{s} \in S^2$, $t \in [0, T]$, we defined functions $\Phi_i : S^2 \times [0, T] \to \mathbb{R}_{\geq 0}$ by $\Phi_i(\vec{s}, t) = \Phi_i(\vec{X}(\vec{s}, t))$.

Molecular interactions

In this model we considered eight different molecular/chemical components Φ_i, denoted by β_cat, β_cat_{ant}, $Wnt3$, $Wnt3_{ant}$, $Head$, SD, $Tent$, and $Tent_{ant}$. For an overview see Table 1. Here, β_cat and β_cat_{ant} represent the activator and the inhibitor associated with the body axis patterning system involving nuclear β-catenin/Tcf. $Wnt3$ and $Wnt3_{ant}$ are the activator and inhibitor of the Wnt3 organizer pattern formation system, respectively. $Head$ is one of several head-specific gene products downstream of the organizer (such as one of the multiple head-specific Wnts [78]), SD denotes the source density, and $Tent$ and $Tent_{ant}$ describe the activator and inhibitor of the tentacle system, respectively. The PDE system describing interactions among these components is given in Eqs. (1)-(7), where $\Delta^{\Gamma}(.)$ denotes the surface Laplace (Laplace–Beltrami) operator, and d_t stands for time-derivative.

More specifically, Eqs. (1)–(2) describe the body axis pattern formation system, Eqs. (3)–(4) describe the organizer pattern formation system, and Eq. (5) describes the equation for $Head$. The tentacle system given by Eqs. (6)–(7) and Eq. (8) for the source density, Eqs. (6)–(8) are adopted from [62, 64]. For the sake of simplicity, we modelled the pattern formation system of β-catenin/Tcf using a system of reaction–diffusion equations, even though β-catenin is a non-diffusive molecule localized in cells. The diffusion-based model is an abstract representation of a more complex pattern formation model in which effective short-range cell-to-cell communication may be realized through interactions with Wnt signalling [3]. A mechanism of pattern formation exhibited by components of intracellular signalling coupled to a single diffusive component has been demonstrated in a series of mathematical works [38, 59]. The desired pattern formation mechanism can be also realized by the interplay between β-catenin and mechanical cues. Such formation of morphogen patterns in the absence of lateral chemical

diffusion has recently been demonstrated in simulation studies based on a mechano-chemical model [16]. Considering several possible molecular mechanisms that could explain the formation of the β-catenin/Tcf patterns, we formulated the current model in terms of a reduced mathematical metaphor for such mechanisms. A similar modelling strategy was applied in the seminal works of Hans Meinhardt [62, 64].

The extension of our model compared with previous models includes a separate activator–inhibitor system for the Wnt3 organizer system and the additional variable $Head$, which represents the head-specific molecules expressed downstream of the organizer in order to fine-scale the pattern of the *Hydra* head region (e.g., multiple Wnts [52]). The activator–inhibitor system for Wnt3 is strictly related to the tentacle system, i.e., a small-scale pattern formation system with saturation of its own expression, motivated by the comparable sizes and spacings of the (transient) Wnt3 spots after ALP treatment, compared with the ectopic tentacles (Fig. 1 b–c). The production terms in the Wnt3 pattern formation system are also assumed to additionally require β-catenin/Tcf, as explained in the Results and Discussion sections. Wnt3 again activates head-specific molecules ($Head$), but only above a certain threshold, $thresh = 5.0$. We introduced this threshold to account for the assumption that head construction only starts if the organizer is well established. $Head$ is again assumed to negatively influence the tentacle system. This negative influence of the *Hydra* hypostomal region on the tentacle system has been demonstrated in different experiments [80, 87, 95].

The large total number of variables/fields in the presented model may lead to the conclusion that that our model has "...so many parameters that they can made to fit anything..." [56]. However, we want to highlight that most parameters in Eqs. (1–8) are not critical for the qualitative simulation results as presented within this study. Notably, most of them control specific properties of one of the three considered *de novo* pattern formation systems, such as spatial scaling in general, spacing between appearing maxima, or the condition required to start the *de novo* patterning process. Most of these parameter have been adopted from Ref. [62, 64]; they are not within the focus of the current study and do not critically influence our main results, the latter concerning the interactions of the different pattern formation systems in *Hydra* rather than the details or the *de novo* pattern formation systems themselves. Detailed molecular mechanisms of the latter are still elusive and need to be worked out, but are beyond the scope of this work. The activator-inhibitor model has thus been used just as an appropriate "toy-model". Therefore, the main aim of this manuscript is to focus on the aspects of *Hydra* patterning that do not dependent of the specific choice of *de novo* patterning mechanisms, but to investigate the existence and interplay of the different patterning systems, rather than searching for specific molecular interactions that could fit to a specific pattern formation mechanism. We thus think that our main conclusions are largely unaffected by most of the model parameters. Since simulation times for our models are not feasible for a systematically numerical robustness analysis, we demonstrated this robustness by developing and simulating an alternative model relying on similar proposed scales and interactions between the distinct pattern formation systems, but realizing *de novo* patterning for each single system in completely different ways. More details are given in the Results and Discussion Section as well as in the supporting information S3.

$$d_t\beta_cat = a_1\Delta^\Gamma\beta_cat + b_1\cdot SD\cdot\frac{0.05+\beta_{cat}^2}{\beta_cat_{ant}} - d_1\cdot\beta_cat \tag{1}$$

$$d_t\,\beta_cat_{ant} = a_2\Delta^\Gamma\beta_cat_{ant} + b_2\cdot SD\cdot\beta_{cat}^2 - d_2\cdot\beta_cat_{ant} \tag{2}$$

$$\begin{aligned} d_tWnt3 = {} & a_3\Delta^\Gamma Wnt3 + b_3\cdot\beta_cat\cdot\frac{0.005+Wnt3^2}{Wnt3_{ant}\cdot(1.0+c_3\cdot Wnt3^2)} - d_3\cdot Wnt3 \\ d_tWnt3_{ant} = {} & a_4\Delta^\Gamma Wnt3_{ant} + b_4\cdot\beta_cat\cdot\frac{0.005+Wnt3^2}{1.0+c_4\cdot Wnt3^2} + 0.06 \\ & -d_4\cdot Wnt3_{ant} \end{aligned} \tag{3}$$

$$d_tHead = a_5\Delta^\Gamma Head - d_5Head + \Big(b_5Wnt3\Big)\Big|_{Wnt3>thresh} \tag{4}$$

$$d_tTent = a_6\Delta^\Gamma Tent + \frac{b_6\cdot SD\cdot(0.005+Tent^2)}{Tent_{ant}\cdot(1+c_6\cdot Tent^2)\cdot(1+e_6\cdot Head)} - d_6\cdot Tent \tag{5}$$

$$d_tTent_{ant} = a_7\Delta^\Gamma Tent_{ant} + \frac{b_7\cdot SD\cdot(0.005+Tent^2)}{(1+c_7\cdot Tent^2)\cdot(1+e_7\cdot Head)} + 0.014 - d_7\cdot Tent_{ant} \tag{6}$$

$$d_t\,SD = a_8\Delta^\Gamma SD + b_8\cdot\beta_cat + 10^{-4} - d_8SD. \tag{7}$$

Tissue mechanics

The chemical/molecular equations Eqs. (1)–(8) have been augmented by a set of equations representing the deforming tissue surface. In particular, we treated the tissue as purely elastic, and elastic tissue deformations are based on minimization of the Helfrich free energy [40], which is given by

$$\mathcal{F}_{bend} = \int_\Gamma \kappa\big(H - H_0(\beta_cat, Tent)\big)^2\, d\vec{S}.$$

Here, H is the mean curvature, κ the bending rigidity, and H_0 the spontaneous curvature [67,70]. H_0 represents the locally preferred tissue curvature, which again may depend on local morphogen concentrations. Here, we assumed $H_0(\beta_cat_{ant}, Tent) = 0.5\cdot\beta_cat_{ant} + 15.\cdot Tent$, based on the observation that local tissue evaginations can be observed during both budding and tentacle formation [1,78]. Local area-conserving evolution of the deforming *Hydra* tissue is finally given by the L^2-gradient flow of the total energy. Further details are given in Ref. [70].

Since the model proposed in this paper focuses on the interplay of pattern formation feedback loops in the biochemical signaling system, simulated changes in tissue curvature are only a read-out of biochemical morphogen concentrations. We include the resulting evolution of the tissue geometry in our model (through a respective partial differential equation describing tissue mechanics), since even dynamics of a purely biochemical model depend on the domain size and geometry that may influence appearance and spacing of the organizing centers. There exist various theoretical studies demonstrating that Turing-type patterns directly depend on the underlying geometry leading, e.g., to spots on the body and stripes on the tail during animal coat patterning. We are, therefore, convinced that the interaction of biochemical patterning and tissue geometry, which is approximating the real geometry, is important to obtain realistic patterns. Among others, this allows for a more realistic description of tentacle formation in our model, which can again be used for further model validation (e.g., simulating ALP treatment).

We demonstrated before [52,78] that Wnt5 and Wnt8 clearly act downstream of canonical Wnt 3 and Wnt9/10 signaling. At least Wnt5 acts as a non-canonical Wnt signal during tentacle formation, and non-canonical Wnts are well known to be involved in planar cell polarity, which in turn is closely linked to changes in cell geometry. Downstream of non-canonical Wnt signaling during tentacle outgrowth, Hydra Alx-spots change from spots to rings [87], most probably resulting from the interplay between chemistry and geometry. Nevertheless, while there is most likely an interplay of chemical signaling with the underlying evolving tissue geometry, strong geometry changes are not considered in the presented paper, as they seem to be irrelevant for the mechanism of axis formation per se.

Simulation method

For simulations of the model we used the finite element library Gascoigne [5], approximating the fourth order PDEs in a mixed formulation. For spatial discretization, we used linear finite elements (including local mesh refinement in areas with strong local curvatures), and for time discretization, we used a semi-implicit Euler scheme (including an adaptive time-step scheme). Further details of the computation scheme are provided in [67, 70].

Parameters and initial conditions

For simulations of the undisturbed system, most of the parameters were adapted from Ref. [62, 64]. For the unperturbed system, we used: $a_1 = 9 \times 10^{-5}, b_1 = d_1 = 3 \times 10^{-3}, a_2 = 1.1 \times 10^{-2}, b_2 = 3 \times 10^{-3}, d_2 = 4 \times 10^{-3}, a_3 = 2.25 \times 10^{-5}, b_3 = 4.8 \times 10^{-2}, c_3 = 1.8 \times 10^{-3}, d_3 = 1.2 \times 10^{-2}, a_4 = 0.9 \times 10^{-3}, b_4 = 0.72 \times 10^{-1}, c_4 = 1.8 \times 10^{-3}, d_4 = 1.8 \times 10^{-2}, a_5 = 5 \times 10^{-4}, d_5 = 1 \times 10^{-2}, b_5 = 1, a_6 = 7.5 \times 10^{-5}, b_6 = 2 \times 10^{-2}, c_6 = e_6 = 1 \times 10^{-1}, d_6 = 2 \times 10^{-2}, a_7 = 3 \times 10^{-3}, b_7 = 3 \times 10^{-2}, c_7 = e_7 = 1 \times 10^{-1}, d_7 = 3 \times 10^{-2}, a_8 = 1.1 \times 10^{-4}, b_8 = d_8 = 1 \times 10^{-4}$. To approximate the *Hydra* shape, initial conditions for X_1, X_2, and X_3 were parameterized over the closed 2D unit-sphere S^2 embedded in 3D space with $X_1(t = 0) \equiv X_2(t = 0) \equiv 0$ and $X_3(t = 0) = 4 \cdot s_3$, thus leading to stretch in the direction of s_3 (given that s_1, s_2, s_3 are Eulerian coordinates of the S^2 surface). For chemicals, we used a stochastic initial distribution based on the standard random generator provided by C++. The only exception was the source density, which was provided with an initial gradient, namely via $SD(t = 0) = 4.0 \cdot (exp(s_3)/exp(1))$. Thus, in all simulations, chemical patterns developed based on stochastic initial conditions, with only the geometric and chemical body axis gradient initially provided. For simulations including ALP treatment, we changed the initial conditions for the source density by adding an offset by $SD(t = 0) = 2.0 + 4.0 \cdot (exp(s_3)/exp(1))$. *Sp5* knockdown was simulated by increasing degradation of $Wnt3_ant$ by multiplying d_4 by the factor 1.7, and overexpression of *β-catenin/Tcf* and *Wnt3* were realized by adding the constant $c = 0.003$ to the right-hand side of the corresponding equation.

Acknowledgements

This work is supported by Deutsche Forschungsgemeinschaft (DFG) under Germany's Excellence Strategy EXC-2181/1 - 390900948 (the Heidelberg STRUCTURES Excellence Cluster) and SFB1324 (B05 to A.M-C and M.M., B07 to SÖ, and A05 to T.W.H). We thank Yukio Nakamura for the preparation of the actin::Wnt3 pBSSA-AR vector and initial transgenic *Hydra vulgaris* AEP strains (DFG-FOR 942; T.W.H).

References

1. R. Aufschnaiter, R. Wedlich-Söldner, X. Zhang, and B. Hobmayer, *Apical and basal epitheliomuscular F-actin dynamics during bud evagination.*, Biol. Open, 6 (2017), pp. 1137–48.
2. R. Augustin, A. Franke, K. Khalturin, R. Kiko, S. Siebert, G. Hemmrich, and T. C. G. Bosch, *Dickkopf related genes are components of the positional value gradient in Hydra.*, Dev. Biol., 296 (2006), pp. 62–70.
3. N. Barker, *The canonical Wnt/beta-catenin signalling pathway.*, Mol. Biol., 468 (2008), pp. 5–15.
4. L. Beccari, N. Moris, M. Girgin, D. A. Turner, P. Baillie-Johnson, A.-C. Cossy, M. P. Lutolf, D. Duboule, and A. M. Arias, *Multi-axial self-organization properties of mouse embryonic stem cells into gastruloids.*, Nature, 562 (2018), pp. 272–276.
5. R. Becker, M. Braack, T. Dunne, D. Meidner, T. Richter, and B. Vexler, *Gascoigne 3D- a finite element toolbox (http://www.gascoigne.uni-hd.de).* 2005.
6. S. Berking, *A model for budding in hydra: pattern formation in concentric rings*, J. Theor. Biol., 222 (2003), pp. 37–52.
7. H. R. Bode, *Head regeneration in Hydra*, Dev. Dyn., 226 (2003), pp. 225–36.
8. H. R. Bode, *Axial patterning in Hydra.*, CSH Perspect. Biol., 1 (2009), p. a000463.
9. H. R. Bode, *Axis formation in Hydra.*, Annu Rev Genet, 45 (2011), pp. 105–17.

10. H. R. Bode, *The head organizer in Hydra.*, Int. J. Dev. Biol., 56 (2012), pp. 473–8.
11. P. M. Bode and H. R. Bode, *Formation of pattern in regenerating tissue pieces of Hydra attenuata. I. Head-body proportion regulation.*, Dev. Biol., 78 (1980), pp. 484–96.
12. T. C. G. Bosch, M. Adamska, R. Augustin, T. Domazet-Loso, S. Foret, S. Fraune, N. Funayama, J. Grasis, M. Hamada, M. Hatta, B. Hobmayer, K. Kawai, A. Klimovich, M. Manuel, C. Shinzato, U. Technau, S. Yum, and D. J. Miller, *How do environmental factors influence life cycles and development? An experimental framework for early-diverging metazoans.*, BioEssays: news and reviews in molecular, cellular and developmental biology, 36 (2014), pp. 1185–94.
13. A. Böttger and M. Hassel, *Hydra, a model system to trace the emergence of boundaries in developing eumetazoans.*, Int. J. Dev. Biol., 56 (2012), pp. 583–91.
14. E. Braun and K. Keren, *Hydra regeneration: Closing the loop with mechanical processes in morphogenesis*, BioEssays, 40 (2018), p. 1700204.
15. E. Braun and H. Ori, *Electric-induced reversal of morphogenesis in hydra regeneration*, Bioph. J., 117 (2019), pp. 1514–1523.
16. F. Brinkmann, M. Mercker, T. Richter, and A. Marciniak-Czochra, *Post-Turing tissue pattern formation: Advent of mechanochemistry.*, PLoS Comput. Biol., 14 (2018), p. e1006259.
17. M. Broun and H. R. Bode, *Characterization of the head organizer in Hydra.*, Development, 129 (2002), pp. 875–84.
18. M. Broun, L. Gee, B. Reinhardt, and H. R. Bode, *Formation of the head organizer in Hydra involves the canonical Wnt pathway.*, Development, 132 (2005), pp. 2907–16.
19. M. Broun, S. Sokol, and H. R. Bode, *Cngsc, a homologue of goosecoid, participates in the patterning of the head, and is expressed in the organizer region of Hydra.*, Development, 126 (1999), pp. 5245–54.
20. E. N. Browne, *The production of new hydranths in Hydra by the insertion of small grafts*, J. Exp. Zool., 7 (1909), pp. 1–23.
21. C. Cramer von Laue, *Untersuchungen zur dualen Funktion von beta-Catenin im Wnt-Signalweg und der Cadherin-vermittelten Zelladhäsion bei Hydra*, PhD thesis, Technische Universität Darmstadt, 2004.
22. W. Driever and C. Nüsslein-Volhard, *A gradient of bicoid protein in drosophila embryos*, Cell, 54 (1988), pp. 83–93.
23. J. Ferenc, P. Papasaikas, J. Ferralli, Y. Nakamura, S. Smallwood, and C. D. Tsiairis, *Wnt3 expression as a readout of tissue stretching during Hydra regeneration*, bioRxiv, doi (2020), p. https://doi.org/10.1101/2020.12.22.423911.
24. A. C. Fröbius, G. Genikhovich, U. Kürn, F. Anton-Erxleben, and T. C. G. Bosch, *Expression of developmental genes during early embryogenesis of Hydra.*, Dev. Genes Evol., 213 (2003), pp. 445–55.
25. B. Galliot, *Hydra, a fruitful model system for 270 years*, Int. J. Dev. Biol., 56 (2012), pp. 411–23.
26. B. Galliot and V. Schmid, *Cnidarians as a model system for understanding evolution and regeneration.*, Int. J. Dev. Biol., 46 (2002), pp. 39–48.
27. A. Gamba, M. Nicodemi, J. Soriano, and A. Ott, *Critical behavior and axis defining symmetry breaking in Hydra embryonic development.*, Phys .Rev. Lett., 108 (2012), p. 158103.
28. M. V. Gammons, M. Renko, J. E. Flack, J. Mieszczanek, and M. Bienz, *Feedback control of Wnt signaling basedon ultrastable histidine cluster co-aggregation between Naked/NKD and Axin*, eLife, 9 (2020), p. e59879.
29. L. Gee, J. Hartig, L. Law, J. Wittlieb, K. Khalturin, and T. Bosch, *Beta-catenin plays a central role in setting up the head organiser in hydra*, Dev. Biol., 340 (2010), pp. 226–24.
30. G. Genikhovich, U. Kürn, G. Hemmrich, and T. C. G. Bosch, *Discovery of genes expressed in hydra embryogenesis.*, Dev. Biol., 289 (2006), pp. 466–81.
31. A. Gierer, *The hydra model - a model for what?*, Int. J. Dev. Biol., 56 (2012), pp. 437–45.

32. A. Gierer, S. Berking, H. Bode, C. David, K. Flick, G. Hansmann, H. Schaller, and E. Trenkner, *Regeneration of hydra from reaggregated cells*, Nature New Biol., 239: 91 (1972), pp. 98–101.

33. A. Gierer and H. Meinhardt, *A theory of biological pattern formation.*, Kybernetik, 12 (1972), pp. 30–9.

34. C. Grimmelikhuijzen and H. Schaller, *Hydra as a model organism for the study of morphogenesis*, TIBS, 4 (1979), pp. 265–7.

35. C. Guder, I. Philipp, T. Lengfeld, H. Watanabe, B. Hobmayer, and T. W. Holstein, *The Wnt code: cnidarians signal the way.*, Oncogene, 25 (2006), pp. 7450–60.

36. C. Guder, S. Pinho, T. G. Nacak, H. A. Schmidt, B. Hobmayer, C. Niehrs, and T. W. Holstein, *An ancient Wnt-dickkopf antagonism in Hydra.*, Development, 133 (2006), pp. 901–11.

37. S. Gufler, B. Artes, H. Bielen, I. Krainer, M.-K. Eder, J. Falschlunger, A. Bollmann, T. Ostermann, T. Valovka, M. Hartl, K. Bister, U. Technau, and B. Hobmayer, *β-Catenin acts in a position-independent regeneration response in the simple eumetazoan Hydra.*, Dev. Biol., 433 (2018), pp. 310–23.

38. S. Härting and A. Marciniak-Czochra, *Spike patterns in a reactiondiffusion ode model with turing instability*, Mathematical Methods in the Applied Science, 37 (2013), pp. 1377–1391.

39. M. Hassel and A. Bieller, *Stepwise transfer from high to low lithium concentrations increases the head-forming potential in Hydra vulgaris and possibly activates the PI cycle.*, Dev. Biol., 177 (1996), pp. 439–48.

40. W. Helfrich, *Elastic properties of lipid bilayers: theory and possible experiments.*, Z Naturforsch [C], 28 (1973), pp. 693–703.

41. B. Hobmayer, F. Rentzsch, K. Kuhn, C. M. Happel, C. C. von Laue, P. Snyder, U. Rothbächer, and T. W. Holstein, *Wnt signalling molecules act in axis formation in the diploblastic metazoan Hydra*, Nature, 407 (2000), pp. 186–9.

42. E. Hobmayer, M. Hatta, R. Fischer, T. Fujisawa, T. W. Holstein, and T. Sugiyama, *Identification of a Hydra homologue of the beta-catenin/plakoglobin/armadillo gene family.*, Gene, 172 (1996), pp. 155–9.

43. T. W. Holstein, *The evolution of the Wnt pathway.*, CSH Perspect. Biol., 4 (2012), p. a007922.

44. T. W. Holstein, E. Hobmayer, and U. Technau, *Cnidarians: an evolutionarily conserved model system for regeneration?*, Dev. Dyn., 226 (2003), pp. 257–67.

45. R. Iachetta, A. Ambrosone, A. Klimovich, J. Wittlieb, G. Onorato, A. Candeo, C. D'andrea, D. Intartaglia, N. Scotti, M. Blasio, A. Tino, A. Bassi, and C. Tortiglione, *Real time dynamics of β-catenin expression during Hydra development, regeneration and wnt signalling activation.*, Int. J. Dev. Biol., 62 (2018), pp. 311–8.

46. V. Kadu, S. S Ghaskadbi, and S. Ghaskadbi, *Induction of secondary axis in hydra revisited: New insights into pattern formation.*, Int. J. Mol. Cell Med., 1 (2012), pp. 11–20.

47. S. Kakugawa, P. F. Langton, M. Zebisch, S. Howell, T.-H. Chang, Y. Liu, T. Feizi, G. Bineva, N. O'Reilly, A. P. Snijders, E. Y. Jones, and J.-P. Vincent, *Notum deacylates wnt proteins to suppress signalling activity*, Nature, 519 (2015), pp. 187–192.

48. ———, *Notum deacylates Wnt proteins to suppress signalling activity*, Nature, 519 (2015), pp. 187–192.

49. T. Käsbauer, P. Towb, O. Alexandrova, C. N. David, E. Dall'armi, A. Staudigl, B. Stiening, and A. Böttger, *The Notch signaling pathway in the cnidarian Hydra.*, Dev. Biol., 303 (2007), pp. 376–90.

50. Y. Komiya and R. Habas, *Wnt signal transduction pathways.*, Organogenesis, 4 (2008), pp. 68–75.

51. L. Leclere, R. R. Copley, T. Momose, and E. Houliston, *Hydrozoan insights in animal development and evolution*, Curr. Opin. Genet. Dev., 39 (2016), pp. 157–67.

52. T. Lengfeld, H. Watanabe, O. Simakov, D. Lindgens, L. Gee, L. Law, H. A. Schmidt, S. Ozbek, H. Bode, and T. W. Holstein, *Multiple Wnts are involved in Hydra organizer formation and regeneration.*, Dev. Biol., 330 (2009), pp. 186–99.

53. A. Livshits, L. Shani-Zerbib, Y. Maroudas-Sacks, E. Braun, and K. Keren, *Structural inheritance of the actin cytoskeletal organization determines the body axis in regenerating Hydra*, Cell Rep., 18 (2017), pp. 1410–21.

54. M. Lommel, J. Strompen, A. L. Hellewell, G. P. Balasubramanian, E. D. Christofidou, A. R. Thomson, A. L. Boyle, D. N. Woolfson, K. Puglisi, M. Hartl, T. W. Holstein, J. C. Adams, and S. Özbek, *Hydra mesoglea proteome identifies thrombospondin as a conserved component active in head organizer restriction.*, Sci. Rep., 8 (2018), p. 11753.

55. M. Lommel, A. Tursch, L. R. Calvo, B. Trageser, and T. W. Holstein, *Genetic knockdown and knockout approaches in hydra*, www.biorxiv.org, (2018).

56. H. K. MacWilliams, *Numerical simulations of hydra head regeneration using a proportion-regulating version of the Gierer-Meinhardt model*, J. Theor. Biol., 99 (1982), pp. 681–703.

57. H. K. MacWilliams, *Hydra transplantation phenomena and the mechanism of hydra head regeneration. I. Properties of the head inhibition.*, Dev. Biol., 96 (1983), pp. 217–38.

58. ———, *Hydra transplantation phenomena and the mechanism of hydra head regeneration. II. Properties of the head activation.*, Dev. Biol., 96 (1983), pp. 239–57.

59. A. Marciniak-Czochra, *Receptor-based models with hysteresis for pattern formation in hydra*, Math. Biosci., 199 (2006), pp. 97–119.

60. ———, *Mathematics and Life Sciences*, Germany: De Gruyter, 2012, ch. Reaction-diffusion models of pattern formation in developmental biology.

61. V. J. Martin, C. L. Littlefield, W. E. Archer, and H. R. Bode, *Embryogenesis in hydra*, Biol. Bull., 192 (1997), pp. 345–63.

62. H. Meinhardt, *A model for pattern formation of hypostome, tentacles, and foot in hydra: how to form structures close to each other, how to form them at a distance*, Dev. Biol., 157 (1993), pp. 321–33.

63. ———, *Models for the generation and interpretation of gradients.*, CSH Perspect. Biol., 1 (2009), p. a001362.

64. ———, *Modeling pattern formation in hydra: A route to understanding essential steps in development.*, Int. J. Dev. Biol., 56 (2012), pp. 447–62.

65. H. Meinhardt, *Turing's theory of morphogenesis of 1952 and the subsequent discovery of the crucial role of local self-enhancement and long-range inhibition*, Interface Focus, 2 (2012), pp. 407–16.

66. H. Meinhardt and A. Gierer, *Pattern formation by local self-activation and lateral inhibition.*, Bioessays, 22 (2000), pp. 753–60.

67. M. Mercker, D. Hartmann, and A. Marciniak-Czochra, *A mechanochemical model for embryonic pattern formation: coupling tissue mechanics and morphogen expression.*, PLoS One, 8 (2013), p. e82617.

68. M. Mercker, T. Holstein, S. Özbek, A. Tursch, and A. Marciniak-Czochra, *How dickkopf molecules and wnt/β-catenin interplay to self-organise the Hydra body axis*, BioRxiv, (2021).

69. M. Mercker, A. Köthe, and A. Marciniak-Czochra, *Mechanochemical symmetry breaking in Hydra aggregates.*, Biophys. J., 108 (2015), pp. 2396–407.

70. M. Mercker, A. Marciniak-Czochra, T. Richter, and D. Hartmann, *Modeling and computing of deformation dynamics of inhomogeneous biological surfaces*, SIAM Journal on Applied Mathematics, 73(5) (2013), pp. 1768–1792.

71. W. A. Müller, *Pattern control in Hydra: basic experiments and concepts*, in Experimental and Theoretical Advances in Biological Pattern Formation, H. Othmner, P. Maini, and J. Murray, eds., Boston: Springer, 1993, pp. 237–253.

72. S. Münder, S. Tischer, M. Grundhuber, N. Büchels, N. Bruckmeier, S. Eckert, C. A. Seefeldt, A. Prexl, T. Käsbauer, and A. Böttger, *Notch-signalling is required for head regeneration and tentacle patterning in Hydra*, Dev. Biol., 383 (2013), pp. 146–57.

73. A. Nagafuchi and M. Takeichi, *Transmembrane control of cadherin-mediated cell adhesion: a 94 kDa protein functionally associated with a specific region of the cytoplasmic domain of E-cadherin*, Cell Regul., 1 (1989), pp. 37–44.

74. Y. Nakamura, C. D. Tsiairis, S. Özbek, and T. W. Holstein, *Autoregulatory and repressive inputs localize Hydra Wnt3 to the head organizer.*, Proc. Natl. Acad. Sci. U S A, 108 (2011), pp. 9137–42.

75. K. Noda, *Reconstitution of dissociated cells of Hydra*, Zoology, 80 (1971), pp. 99–101.

76. J. J. Otto and R. D. Campbell, *Budding in Hydra attenuata: bud stages and fate map*, J. Exp. Zool. A Ecol. Genet. Physiol., 200 (1977), pp. 417–28.

77. C. P. Petersen and P. W. Reddien, *Wnt signaling and the polarity of the primary body axis*, Cell, 139 (2009), pp. 1056–68.

78. I. Philipp, R. Aufschnaiter, S. Özbek, S. Pontasch, M. Jenewein, H. Watanabe, F. Rentzsch, T. W. Holstein, and B. Hobmayer, *Wnt/beta-catenin and noncanonical Wnt signaling interact in tissue evagination in the simple eumetazoan Hydra*, Proc. Natl. Acad. Sci. U S A, 106 (2009), pp. 4290–5.

79. P. C. Reddy, A. Gungi, S. Ubhe, S. J. Pradhan, A. Kolte, and S. Galande, *Molecular signature of an ancient organizer regulated by Wnt/β-catenin signalling during primary body axis patterning in Hydra*, Commun. Biol., 2 (2019).

80. B. Reinhardt, M. Broun, I. L. Blitz, and H. R. Bode, *HyBMP5-8b, a BMP5-8 orthologue, acts during axial patterning and tentacle formation in hydra.*, Dev. Biol., 267 (2004), pp. 43–59.

81. R. Rousset, J. A. Mack, K. A. Wharton, J. D. Axelrod, K. M. Cadigan, M. P. Fish, R. Nusse, and M. P. Scott, *Naked cuticle targets dishevelled to antagonize Wnt signal transduction*, Genes Dev, 15 (2001), pp. 658–671.

82. H. Sander, *Symmetry breaking in regenerating hydra: The role of fluctuations and cell mechanics*, PhD thesis, Saarland University, 2016.

83. M. Sato, H. Tashiro, A. Oikawa, and Y. Sawada, *Patterning in hydra cell aggregates without the sorting of cells from different axial origins.*, Dev. Biol., 151 (1992), pp. 111–6.

84. F. Schweisguth and F. Corson, *Self-organization in pattern formation.*, Dev. Cell, 49 (2019), pp. 659–77.

85. J. A. Sherratt, P. Maini, W. Jäger, and W. Müller, *A receptor based model for pattern formation in Hydra*, Forma, 10 (1995), pp. 77–95.

86. H. Shimizu, *Transplantation analysis of developmental mechanisms in Hydra*, Int. J. Dev. Biol., 56 (2012), pp. 463–72.

87. K. M. Smith, L. Gee, and H. R. Bode, *HyAlx, an aristaless-related gene, is involved in tentacle formation in hydra*, Development, 127 (2000), pp. 4743–52.

88. J. Soriano, C. Colombo, and A. Ott, *Hydra molecular network reaches criticality at the symmetry-breaking axis-defining moment.*, Phys Rev Lett, 97 (2006), p. 258102.

89. J. Soriano, S. Rüdiger, P. Pullarkat, and A. Ott, *Mechanogenetic coupling of Hydra symmetry breaking and driven Turing instability model.*, Biophys. J., 96 (2009), pp. 1649–60.

90. R. E. Steele, *Trembley's polyps go transgenic*, Proc. Natl. Acad. Sci. U S A, 103 (2006), pp. 6415–6.

91. J. Taubenheim, D. Willoweit-Ohl, M. Knop, S. Franzenburg, T. C. Bosch, and S. Fraune, *Bacteria-and temperature-regulated peptides modulate beta-catenin signaling in hydra*, bioRxiv, doi (2019), p. https://doi.org/10.1101/7473.

92. U. Technau and H. R. Bode, *HyBra1, a Brachyury homologue, acts during head formation in Hydra*, Development, 126 (1999), pp. 999–1010.

93. U. Technau, C. Cramer von Laue, F. Rentzsch, S. Luft, B. Hobmayer, H. R. Bode, and T. W. Holstein, *Parameters of self-organization in Hydra aggregates.*, Proc. Natl. Acad. Sci. U S A, 97 (2000), pp. 12127–31.

94. U. Technau and T. W. Holstein, *Cell sorting during the regeneration of Hydra from reaggregated cells*, Dev. Biol., 151 (1992), pp. 117–27.

95. ———, *Head formation in Hydra is different at apical and basal levels*, Development, 121 (1995), pp. 1273–82.

96. S. Tomczyk, K. Fischer, S. Austad, and B. Galliot, *Hydra, a powerful model for aging studies*, Invertebrate Reproduction and Development, 59 (2005), pp. 11–16.

97. A. Trembley, *Mémoires pour servir à l'histoire d'un genre de polypes d'eau douce, à bras en forme de cornes*, vol. 1, Chez Jean & Herman Verbeek, 1744.

98. V. Trivedi, T. Fulton, A. Attardi, K. Anlas, C. Dingare, A. Martinez-Arias, and B. Steventon, *Self-organised symmetry breaking in zebrafish reveals feedback from morphogenesis to pattern formation*, BioRxiv, (2019), p. 769257.

99. A. M. Turing, *The chemical basis of morphogenesis.*, Phil. Trans. R. Soc. Lond. B, 237 (1953), pp. 37–72.

100. D. A. Turner, P. Baillie-Johnson, and A. Martinez Arias, *Organoids and the genetically encoded self-assembly of embryonic stem cells.*, BioEssays, 38 (2016), pp. 181–91.

101. D. A. Turner, M. Girgin, L. Alonso-Crisostomo, V. Trivedi, P. Baillie-Johnson, C. R. Glodowski, P. C. Hayward, J. Collignon, C. Gustavsen, P. Serup, et al., *Anteroposterior polarity and elongation in the absence of extra-embryonic tissues and of spatially localised signalling in gastruloids: mammalian embryonic organoids*, Development, 144 (2017), pp. 3894–3906.

102. M. Veschgini, H. O. Petersen, W. Abuillan, F. F. Rossetti, S. Özbek, M. Burghammer, T. W. Holstein, and M. Tanaka, *Spatio-temporal elasticity patterns in extracellular matrix during hydra morphogenesis*, bioRxiv, doi (2017), p. https://doi.org/10.1101/214718.

103. M. C. Vogg, L. Beccari, L. Iglesias Oll. Rampon, S. Vriz, C. Perruchoud, Y. Wenger, and B. Galliot, *An evolutionarily-conserved Wnt3/β-catenin/Sp5 feedback loop restricts head organizer activity in Hydra*, Nat. Commun., 10 (2019), p. 312.

104. M. C. Vogg, B. Galliot, and C. D. Tsiairis, *Model systems for regeneration: Hydra*, Development, 146 (2019), p. https://doi.org/10.1242/dev.177212.

105. A. Wagner, *Distributed robustness versus redundancy as causes of mutational robustness*, Bioessays, 27 (2005), pp. 176–88.

106. H. Watanabe, H. A. Schmidt, A. Kuhn, S. K. Höger, Y. Kocagöz, N. Laumann-Lipp, S. Özbek, and T. W. Holstein, *Nodal signalling determines biradial asymmetry in hydra*, Nature, 515 (2014), pp. 112–5.

107. S. Werner, H. T.-K. Vu, and J. C. Rink, *Self-organization in development, regeneration and organoids*, Curr. Opin. Cell Biol., 44 (2017), pp. 102–9.

108. K. A. Wharton, G. Zimmermann, R. Rousset, and M. P. Scott, *Vertebrate proteins related to drosophila naked cuticle bind dishevelled and antagonize wnt signaling*, Dev Biol., 234 (2001), pp. 93–106.

109. J. Wittlieb, K. Khalturin, J. U. Lohmann, F. Anton-Erxleben, and T. C. G. Bosch, *Transgenic hydra allow in vivo tracking of individual stem cells during morphogenesis.*, Proceedings of the National Academy of Sciences of the United States of America, 103 (2006), pp. 6208–6211.

110. L. Wolpert, *Positional information and the spatial pattern of cellular differentiation.*, J. Theor. Biol., 25 (1969), pp. 1–47.

111. L. Wolpert, M. R. Clarke, and A. Hornbruch, *Positional signalling along Hydra.*, Nature, 239 (1972), pp. 101–5.

112. T. Yao, *Studies on the organizer problem in Pelmatohydra oligactis: I. the induction potency of the implants and the nature of the induced hydranth*, J. Exp. Biol., 21 (1945), pp. 147–50.

113. X. Zhang, J. G. Abreu, C. Yokota, B. T. MacDonald, S. Singh, K. L. A. Coburn, S.-M. Cheong, M. M. Zhang, Q.-Z. Ye, H. C. Hang, H. Steen, and X. He, *Tiki1 is required for head formation via Wnt cleavage-oxidation and inactivation*, Cell, 149 (2012), pp. 165–177.

114. B. Ziegler, I. Yiallouros, B. Trageser, S. Kumar, M. Mercker, S. Kling, M. Fath, U. Warnken, M. Schnölzer, T. W. Holstein, M. Hartl, A. Marciniak-Czochra, J. Stetefeld, W. Stöcker, and S. Özbek, *A Wnt-specific astacin proteinase controls head formation in Hydra*, biorxiv.org, (2020).